7 Results: QENS

7.1 Fitting of the theoretical scattering function to the spectra of water

The model employed for the description of the QENS spectra of water contains the following parameters for describing the quasielastic scattering component: the translational diffusion coefficient $D_{TR\,W}$, the residence time between the successive jumps $\tau_{TR\,W}$, the rotational diffusion coefficient $D_{r\,W}$, the mean square displacement $\langle u^2 \rangle_W$. Inelastic scattering was accounted for by the damped harmonic oscillator (DHO) term, see eqs. (5.8, 5.9), with the following parameters: the energy E_{DHO}, damping constant Γ_{DHO} and the mean square displacement $\langle u^2 \rangle_{DHO}$. The spectra of water analyzed in the present work were recorded with different energy resolutions. An attempt was made, therefore, to utilize the scheme outlined in section 5.10 and to determine, as unambiguously as possible, the values of all model parameters.

This attempt was not successful for one main reason: for water, in order to discriminate between the different kinds of motion, QENS spectra with energy resolutions, ΔE, in the range from 1 μeV to >100-200 μeV must be analyzed; the range of the elastic momentum transfer, Q_{EL}, must be broad too (perhaps at least 0.2 $Å^{-1}$ - 4.0 $Å^{-1}$). For the QENS spectra analyzed in this work, the highest ΔE value was about 90 μeV; thus, it was hard to discriminate between rotational and vibrational motions. The maximum value of Q_{EL} was about 2.3 $Å^{-1}$, which made the determination of the parameters of vibrational motions difficult.

In the course of the analysis of the available QENS spectra of water, the following fit parameters were not completely independent and sometimes strongly correlated: $\tau_{TR\,W}$, $D_{r\,W}$, $\langle u^2 \rangle_W$, E_{DHO}, Γ_{DHO} and $\langle u^2 \rangle_{DHO}$. Therefore, in the fits of the water model to the spectra, the following values were arbitrarily fixed for both, H_2O and D_2O, and at all temperatures: E_{DHO}=6 meV and Γ_{DHO}=11 meV, $\langle u^2 \rangle_W$=0.078 $Å^2$. (For comparison, the value of $\langle u^2 \rangle_W$ was reported to be temperature independent and equal to ≈0.077 $Å^2$ [132].) The values of $D_{r\,W}$ were fixed to those obtained in the study of Teixeira et al. [132], $D_{r\,W}(T) = 2.26 \times \exp(-E_a/T)$ [meV], where T is absolute temperature and the activation energy E_a is 1.85 kcal/mol (for example, for T=298 K, $D_{r\,W}$ =0.1 meV).

The parameters $\tau_{TR\,W}$ and $\langle u^2 \rangle_{DHO}$ for D_2O and H_2O were determined in the fits to the D_2O {NEAT(4)} and H_2O {IN5(2)} spectra, respectively; the results are given in Tab. 7.1. Note that the values of $\langle u^2 \rangle_{DHO}$ determined by fitting to the D_2O {NEAT(4)} spectra are decreasing as the temperature increases. This is in apparent contradiction with the fact that the mean square

displacement $\langle u^2 \rangle$ of vibrational motion increases with temperature. Since the primary goal of the analysis of QENS spectra of water was to account for the bulk water contribution to the QENS spectra of solutions, no interpretation of such a result was attempted, crucial was the overall quality of fitting the QENS spectra of water.

In the fits to all solutions and water spectra $\tau_{TR\,W}$ and $\langle u^2 \rangle_{DHO}$ were fixed to the values found by the interpolation of the values from Tab. 7.1 to the desirable temperatures. An Arrhenius law was assumed to hold for $(1/\tau_{TR\,W})$; the $\langle u^2 \rangle_{DHO}$ values were interpolated using the quadratic expression.

Table 7.1 **Parameter values as determined from fitting of the theoretical model to the spectra of D_2O and H_2O.** T – absolute temperature, $\tau_{TR\,W}$ – the mean residence time between the successive jumps, $\langle u^2 \rangle_{DHO}$ - the mean square displacement of the damped harmonic oscillator. For details of the model see section 5.4.

H_2O {IN5(2)}			D_2O {NEAT(4)}		
T [K]	$\tau_{TR\,W}$ [ps]	$\langle u^2 \rangle_{DHO}$ [Å^2]	T [K]	$\tau_{TR\,W}$ [ps]	$\langle u^2 \rangle_{DHO}$ [Å^2]
280	1.16±0.03	0.00671±1.3×10^{-4}	280	1.07±0.02	0.00463±1.0×10^{-4}
290	0.81±0.02	0.00650±1.0×10^{-4}	298	0.54±0.01	0.00409±1.1×10^{-4}
303	0.6±0.02	0.00662±1.1×10^{-4}	316	0.40±0.01	0.00354±1.2×10^{-4}
317	0.53±0.02	0.00712±1.7×10^{-4}	-	-	-

It was recently found (February 2007) that the implementation of eq. (5.9) in the computer program lacked the factor $1/k_BT$ (for T 298 K $1/k_BT = 0.039$ meV^{-1}). The factor $\{\exp(\langle u^2 \rangle_{DHO} Q^2) - 1\}$ from eq. (5.8) is approximately equal to "$\langle u^2 \rangle_{DHO} Q^2$" for small "$\langle u^2 \rangle_{DHO} Q^2$" values. Thus, the lacking factor $1/k_BT$ led to $\langle u^2 \rangle_{DHO}$ values (in Tab. 7.1), which are by the factor $\approx 1/0.039 = 25$ lower than they should be. In fits with the corrected program, $\langle u^2 \rangle_{DHO}$ values were in the range 0.07 – 0.1 Å^2. Apart from the different $\langle u^2 \rangle_{DHO}$ values, the mistake didn't lead to any significant errors.

7.2 QENS spectra of water: examples

Examples of the spectra of D_2O and H_2O recorded with energy resolution in the range 1 μeV – 90 μeV, and fits of $S_{THEO\,W}(Q, \omega)$ to these spectra are given in Figs. A1 – A10 (Appendix A). Generally, the description of the spectra by the fitted curves is satisfactory.

It is seen that with increasing energy resolution (i.e. decreasing ΔE), the statistical errors of the $S_{TOTAL\,W}(Q, \omega)$-data become larger. This is mainly due to the fact that generally, on a given spectrometer, a decrease of ΔE results in a reduction of the incident neutron flux, which is only partially compensated by a longer measurement time.

In the experiment with IN5 the thickness of the H_2O sample was 0.6 mm, so that the

sample transmission was low (T_S = 0.67) and, predictably, the multiple scattering ($S_{MSC\ THEO}$) component is especially substantial, see Figs. A9, A10. Note that, because $S_{MSC\ THEO}$ was only evaluated for a small number of points ω_i and found by interpolation for all others (see Appendix E), sometimes the $S_{MSC\ THEO}$ curves are not smooth functions of ω (e.g. Figs. A8, A10).

Regarding the description of pure water spectra: for small scattering angles the wings on both sides of the quasielastic peak are not ideally described by the fitted curve. This is, at least partially, due to the multiple scattering component, which is only approximated but not precisely reproduced by the approach used in the present work. An indirect evidence for this is that with increasing scattering angle φ, the "wings" are increasingly better fitted. Qualitatively, this can be explained by the fact that at small scattering angles the intensity of multiple scattering in the region $\hbar\omega > 1 - 2$ meV is comparable to the single scattering intensity (and sometimes even higher). Consequently, errors in the determination of the $S_{MSC\ THEO}$ component at small angles lead to an underestimation of the "wings".

7.3 QENS spectra of water: the scaling factor

In section 5.3 a Q_{EL}-dependent scaling factor Sc.F(Q_{EL}) was introduced. Ideally, Sc.F(Q_{EL}) must be Q_{EL}-independent and equal to $V_S \times C$, the factor C is given by eq. (2.54) and V_S is the sample volume exposed to the incident beam. For comparison, values of Sc.F(Q_{EL}) are presented in Fig. 7.1 that were found from fits to a number of D_2O and H_2O spectra.

The dip in Sc.F(Q_{EL}) in Fig. 7.1a,c is caused by the imperfect correction for the factor $H_1(\boldsymbol{k}_0, \boldsymbol{k})$. For the sample angle α (α =45° here) the condition $\varphi = \alpha$ and eq. (2.45) gives Q_{EL} value of 0.94 Å^{-1}, and one can see that the dip in Sc.F(Q_{EL}) is not far from this value (Fig. 7.1a,c). In Fig. 7.1d Sc.F(Q_{EL}) decreases for $Q_{EL} > 1.0$, because the scattering angle φ approaches the sample angle α (Fig. 7.1b,d; α=135°), the condition $\varphi = \alpha$ gives a minimum in Sc.F(Q_{EL}) at Q_{EL}=1.5 Å^{-1}.

The fact that Sc.F(Q_{EL}) increases for $Q_{EL} > 1.2$ Å^{-1} in Fig. 7.1b is explained by the increase of the "unaccounted" scattering from D_2O for $Q_{EL} > 1.0$ Å^{-1}. Such "unaccounted" scattering causes the increase in the Sc.F(Q_{EL}) in Fig. 7.1a for $Q_{EL} > 1.2$ Å^{-1} - 1.4 Å^{-1} as well. (Note that in Fig. 7.1b the effect of the imperfect correction for the factor $H_1(\boldsymbol{k}_0, \boldsymbol{k})$, which led to decrease in Sc.F(Q_{EL}) in Fig. 7.1d, is masked by the "unaccounted" scattering from D_2O.) Clearly, the used expression for $S_{THEO\ W}(Q, \omega)$ underestimates intensity of D_2O scattering for $Q > 1$ Å^{-1}. Consequently, when fitting a model to the spectra of D_2O solutions, eq. (5.3) must be used rather than eq. (5.2); and in fits to QENS spectra of D_2O solutions, Sc.F$_W$(Q_{EL}) must be fixed at the values of Sc.F(Q_{EL}) found in the fits to pure D_2O spectra.

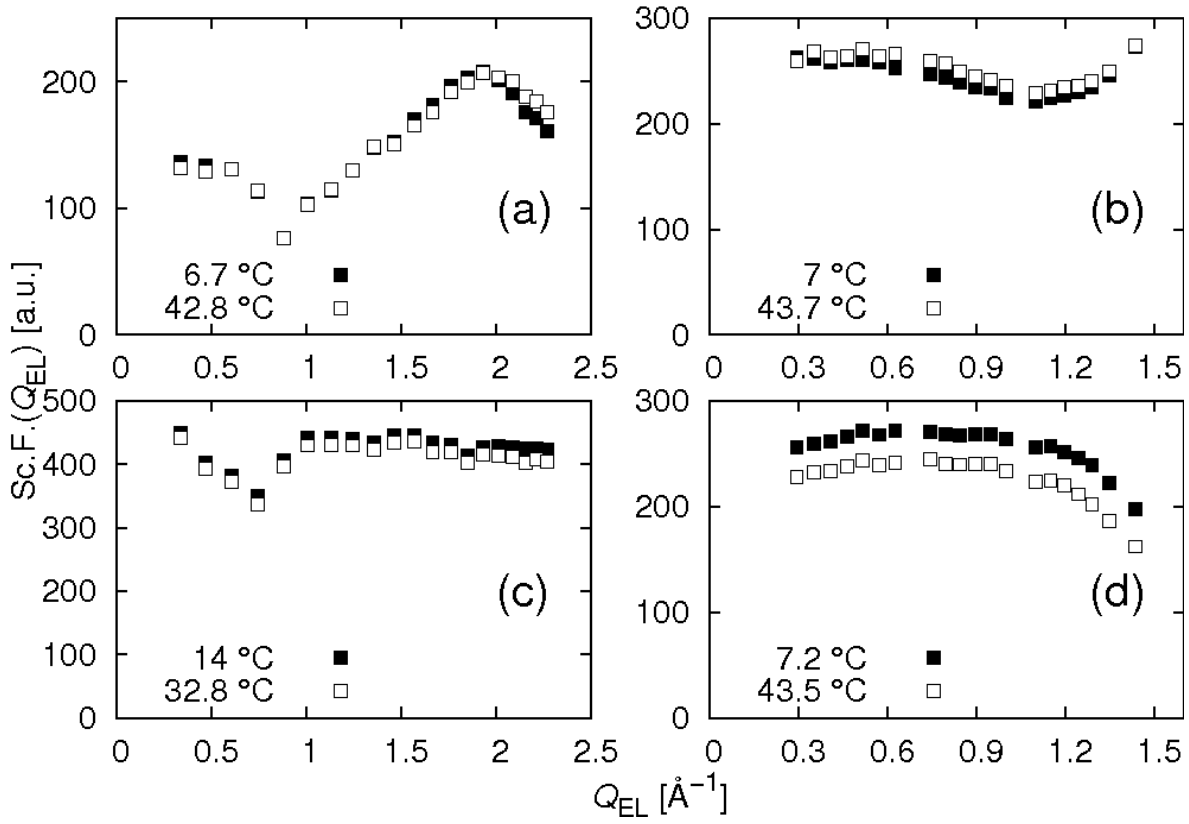

Figure 7.1 **Scaling factor Sc.F(Q_{EL}) determined in the fits to QENS spectra of D_2O and H_2O. (a):** D_2O {NEAT(4)} spectra, λ_0=5.1 Å, $\Delta E \approx 90$ μeV, α=45°; **(b):** D_2O {IN5(1)} spectra, λ_0=7.6 Å, $\Delta E \approx 30$ μeV, α=135°; **(c):** H_2O {NEAT(2)} spectra, λ_0=5.1 Å, $\Delta E \approx 90$ μeV, α=45°; **(d):** H_2O {IN5(2)} spectra, λ_0=7.6 Å, $\Delta E \approx 30$ μeV, α=135°.

The reason for the underestimation of the scattering by D_2O for $Q > 1$ Å^{-1} by $S_{THEO\,W}(Q, \omega)$ may be that the convolution approximation fails (see section 5.7), or the employed values of $S_{D2O}(Q)$ are not correct.

7.4 Concluding remarks on the QENS spectra of water

In water the translational and rotational motions are coupled and $\tau_{TR\,W}$ and $\tau_{ROT\,W}$ are of the same order of magnitude. Good quality of fitting can be obtained with various combinations of $\tau_{TR\,W}$ and $\tau_{ROT\,W}$, illustrating the fact that one can not speak of separate rotational and translational motions in water. Thus, from the practical point of view, it is justified, that in fitting of the water model to the D_2O spectra the rotational diffusion constant $D_{r\,W}$ were fixed at those obtained in the study [132] for H_2O.

The inelastic contribution to QENS spectra of water is substantial for ΔE =30 and 90 μeV. At least for an energy resolution $\Delta E \geq 90$ μeV, it is not trivial to obtain an unambiguous decomposition of the spectrum into the quasielastic and inelastic components. There are reports on the presence of a broad peak in Raman and QENS spectra of water with a maximum at about

6 - 8 meV [73,87,103,134,135]. Regarding the damping constant of the DHO term, values in the range 10 meV - 20 meV were reported (e.g. [134,135]). In attempts to fit spectra of water with 30 μeV and 90 μeV energy resolution, it was found that various combinations of E_{DHO} and Γ_{DHO} values (with E_{DHO} in the range 5 meV - 8 meV and Γ_{DHO} in the range 9 meV - 20 meV) provided a similar fit quality. Therefore, it was a reasonable choice to fix E_{DHO} and Γ_{DHO} to a pair of values belonging to these ranges; thus, E_{DHO} and Γ_{DHO} were fixed at 6 and 11 meV, respectively, for all temperatures.

The results of fitting the expression for $S_{THEO\,W}(Q, \omega)$ to the spectra of D_2O and H_2O allowed to describe the scattering component of the bulk water in the analysis of spectra of aqueous solutions. Thus, the approximations and decisions made in the analysis of the QENS spectra of water are justified *a posteriori*. Nevertheless, an unambiguous determination (in the frame of the model chosen) of structural and dynamical parameters describing QENS spectra of water remains to be a challenging task.

7.5 High resolution QENS spectra of DIMEB solution in heavy water

According to the outline given in section 5.10, the 1 μeV energy resolution spectra were analyzed first. Before presenting the results of fitting the "standard solute model", it is worth to show, that with 1 μeV resolution it is possible to observe the translational and rotational motion of cyclodextrins.

If one approximates the DIMEB molecule by a sphere of radius 8 Å, the translational and rotational diffusion coefficients, $D_{TR\,SOL}$ and $D_{r\,SOL}$, can be estimated, respectively, from the Einstein-Stokes relation:

$$D_{TR} = k_B \times T/6\pi \times \eta \times R \tag{7.1}$$

and from the Debye-Stokes-Einstein relation, (rotation of a sphere) see e.g. [35]:

$$D_r = k_B \times T/6 \times \eta \times V \tag{7.2}$$

For 25 °C and solution in D_2O (viscosity η is taken from [20]) the following values are obtained: $D_{TR\,SOL} \approx 0.25 \times 10^{-5}$ cm^2/s and $D_{r\,SOL} \approx 0.12$ μeV. The rotational correlation time $\tau_{ROT\,SOL}$ is therefore 900 ps, as found from:

$$\tau_{ROT\,SOL}\,[\text{ps}] = 0.6583/6 \times D_{r\,SOL}[\text{meV}] \tag{7.3}$$

It is remarkable that in a number of studies values of translational diffusion coefficients [48,39, 75,91,98,101,138,141] and rotational correlation times [7,9,94,137] for CDs are reported that are similar to the estimates made above.

Specifically, in [75] for β-CD, (concentration 3.81 mg/mL in H_2O) $D_{TR\,SOL}$ values are reported [10^{-5}/cm^2/s]: 0.1492, 0.2274, 0.3224 and 0.4362 for 1, 13, 25 and 37 °C, respectively. For DIMEB, the hydrodynamic radius was found to be 7.9 Å [39], so that the $D_{TR\,SOL}$ value at

infinite dilution is 0.227×10^{-5} cm^2/s at 13 °C, as evaluated from eq. (7.1). In the work [94], for β-CD the rotational correlation time was found to be ≈700 and ≈200 ps at 273 and 333 K, respectively (corresponding to $D_{r\,SOL}$ values of 0.16 and 0.55 μeV, respectively); the concentration of β-CD was ≈14.4 mg/mL in 0.1 M phosphate buffer.

The value of $D_{TR\,SOL}$ equal to 0.1×10^{-5} cm^2/s for the $S_{TR}(Q, \omega)$ from eq. (5.12) and Q =0.2 Å^{-1} provides translational spectral broadening, $FWHM_{TR}$, equal to ≈ 0.53 μeV, see Tab. 7.2 for more $FWHM_{TR}$ values. The value of $D_{r\,SOL}$ = 0.1 μeV corresponds to the rotational spectral broadening, $FWHM_{ROT}(l)$, for l = 1, being 0.4 μeV, see Tab. 7.3 for more $FWHM_{ROT}(l)$ values. Thus, in the experiment with ΔE ≈ 1 μeV {IN16}, one might well expect that a quasielastic broadening due to translational and rotational motion can be observed (because the values of $FWHM_{TR}$ and $FWHM_{ROT}(l)$ will be similar to (or greater than) ΔE).

In a first step, it was assumed that the rotation of DIMEB is too slow to manifest itself in the {IN16} spectra. Therefore, the fit of the "standard solute model" was made with $D_{r\,SOL}$=0 both for DIMEB 39.8 mM and 20.3 mM concentrations. The resulting values of diffusion coefficients together with $D_{TR\,SOL}$ values measured by D. Leitner by means of pulsed field gradient NMR (PFG-NMR) (to be published in [61]) are given in Fig. 7.2 and Tab. 7.4.

Table 7.2 **Magnitudes of the translational spectral broadening (example).** $FWHM_{TR} = 2\times0.06581\times D_{TR\,SOL}Q^2$, $D_{TR\,SOL}$ is the translational diffusion coefficient, here $D_{TR\,SOL}=0.1\times10^{-5}$ cm^2/s

Q [Å^{-1}]	$FWHM_{TR}$ [μeV]
0.1	0.13
0.2	0.53
0.3	1.18
0.5	3.29
0.75	7.4
1.0	13.16
1.25	20.57
1.5	29.61
1.75	40.31
2.0	52.65
2.25	66.63

Table 7.3 **Magnitudes of the rotational spectral broadening (example).** $FWHM_{ROT}(l) = 2\times l(l+1)\times D_{r\,SOL}$, $D_{r\,SOL}$ is the translational diffusion coefficient, here $D_{r\,SOL}$ =0.1 μeV

l	$l(l+1)$	$FWHM_{ROT}(l)$ [μeV]
0	0	0
1	2	0.4
2	6	1.2
3	12	2.4
4	20	4.0
5	30	6.0
6	42	8.4
7	56	11.2
8	72	14.4
9	90	18.0
10	110	22.0

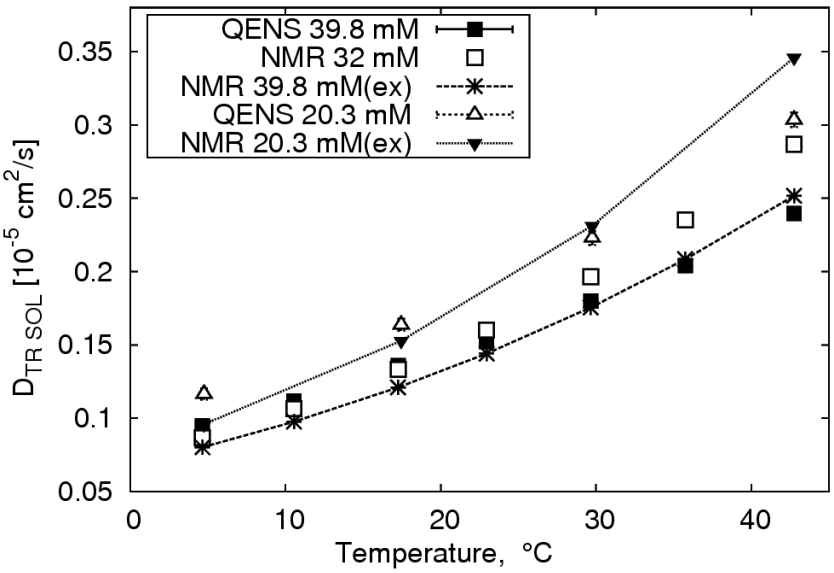

Figure 7.2 **Values of $D_{TR\,SOL}$ for DIMEB solutions in D_2O as obtained from QENS and PFG-NMR experiments.** The "standard solute model" was fitted to DIMEB solutions (39.8 and 20.3 mM) {IN16} spectra, the rotational motion of DIMEB-molecule was neglected; $Q \leq 0.43$ Å^{-1}. PFG-NMR values for concentrations 20.3 mM and 39.8 mM were obtained by extrapolation of PFG-NMR values for 0.1, 1 and 32 mM; the abbreviation "(ex)" stands for "extrapolated values".

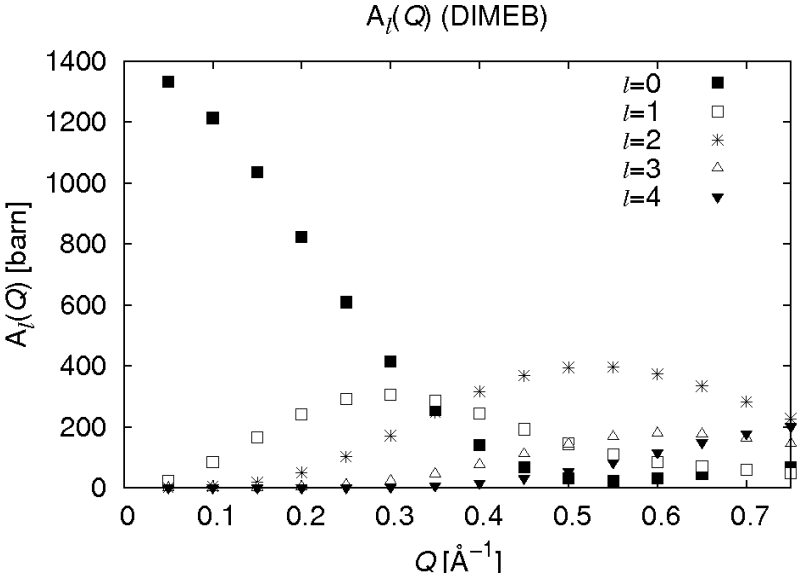

Figure 7.3 **Values of the rotational structure factors, $A_l(Q)$, for DIMEB.** The $A_l(Q)$ values were evaluated using the atomic coordinates from the crystallographic structure of a DIMEB hydrate from eq. (5.17); see section 5.5 for details. For a given l value, $A_l(Q)$ is the weight factor of the solute scattering component with a rotational broadening, FWHM$(l)_{ROT}$, FWHM$(l)_{ROT}$ =2l(l+1)$D_{r\,SOL}$, where $D_{r\,SOL}$ is the solute rotational diffusion coefficient. Clearly, the solute scattering components with non-zero rotational broadening can not be neglected for $Q > 0.3$ Å^{-1}.

Unfortunately, PFG-NMR values for only three concentrations of DIMEB are available: 0.1, 1.0 and 32 mM; therefore, PFG-NMR $D_{TR\ SOL}$ values for 20.3 and 39.8 mM were found using the equation:

$$\ln(D_{TR\ SOL}) = a + b \times c \qquad (7.4)$$

where c is the concentration [mg/mL], "a" and "b" are the coefficients determinedby fitting of eq. (7.4) to available PFG-NMR data and used to evaluate $D_{TR\ SOL}$ for DIMEB at arbitrary concentrations.

One can see (Fig. 7.2) that the values found in the fit to QENS spectra are similar to the extrapolated NMR values. Such an (although not perfect) agreement is intriguing, because, as shown in Fig. 7.3, the contribution of rotational motion to the spectral broadening can *not* be neglected. In Fig. 7.3, the rotational structure factors, $A_l(Q)$, for DIMEB-molecule are plotted. For a given l value, $A_l(Q)$ is the weight factor of the solute scattering component with a rotational broadening, $FWHM(l)_{ROT}$, $FWHM(l)_{ROT} = 2l(l+1)D_{r\ SOL}$. As seen from Fig. 7.3, the DIMEB scattering components with non-zero rotational broadening (i.e. for $l>0$) can not be neglected for $Q > 0.3$ Å^{-1}.

Table 7.4 **Values of translational diffusion coefficients of DIMEB in D_2O solutions as determined by QENS and PFG-NMR.** Fits of the "standard solute model" to the QENS spectra of DIMEB 20.3 and 39.8 mM D_2O solutions were done with $D_{r\ SOL}=0$. PFG-NMR values for 20.3 and 39.8 mM D_2O solutions of DIMEB (abbreviated as "ex. NMR") were found by the extrapolation of the available PFG-NMR values for 0.1, 1 and 32 mM. Dimension of $D_{TR\ SOL}$: [10^{-5} cm^2/s].

DIMEB 39.8 mM			DIMEB 20.3 mM		
t °C	$D_{TR\ SOL}$(QENS)	$D_{TR\ SOL}$ (ex. NMR)	t °C	$D_{TR\ SOL}$ (QENS)	$D_{TR\ SOL}$ (ex. NMR)
4.7	0.0950±0.002	0.0802	4.8	0.117±0.004	0.096
10.6	0.112±0.002	0.0977	17.5	0.164±0.004	0.153
17.3	0.136±0.002	0.121	29.8	0.223±0.005	0.231
23.0	0.152±0.002	0.144	42.8	0.304±0.005	0.346
29.7	0.180±0.003	0.175	-	-	-
35.8	0.204±0.003	0.208	-	-	-
42.8	0.240±0.003	0.252	-	-	-

Note that only the first 2 - 3 scattering angles of {IN16} spectra were used for fitting, and the corresponding Q_{EL} values are 0.19, 0.29 and 0.43 Å^{-1} (for small energy transfers, as is the case in {IN16} spectra, $Q \approx Q_{EL}$). For such Q values, at least $A_1(Q)$ and $A_2(Q)$ can not be neglected (Fig. 7.3), and the corresponding $FWHM_{ROT}$ is 0.4 and 1.2 μeV, respectively, for $D_{r\ SOL}$ =0.1 μeV (Tab. 7.3). Therefore, neglecting rotation *must* lead to overestimated $D_{TR\ SOL}$ values. Surprisingly, at least for temperatures above 25 °C it is not so, when judging by the

results in Fig. 7.2.

It was attempted to fit the {IN16} spectra with $D_{r\,SOL}$ fixed to several different values in the range 0.1- 0.5 μeV; predictably, with $D_{r\,SOL}$ values becoming larger, the resulting $D_{TR\,SOL}$ values became increasingly underestimated (Fig. 7.4).

An attempt to fit {IN16} spectra having both $D_{r\,SOL}$ and $D_{TR\,SOL}$ as free parameters led to $D_{r\,SOL}$ values about 0.2-0.4 μeV and to the underestimated $D_{TR\,SOL}$ values.

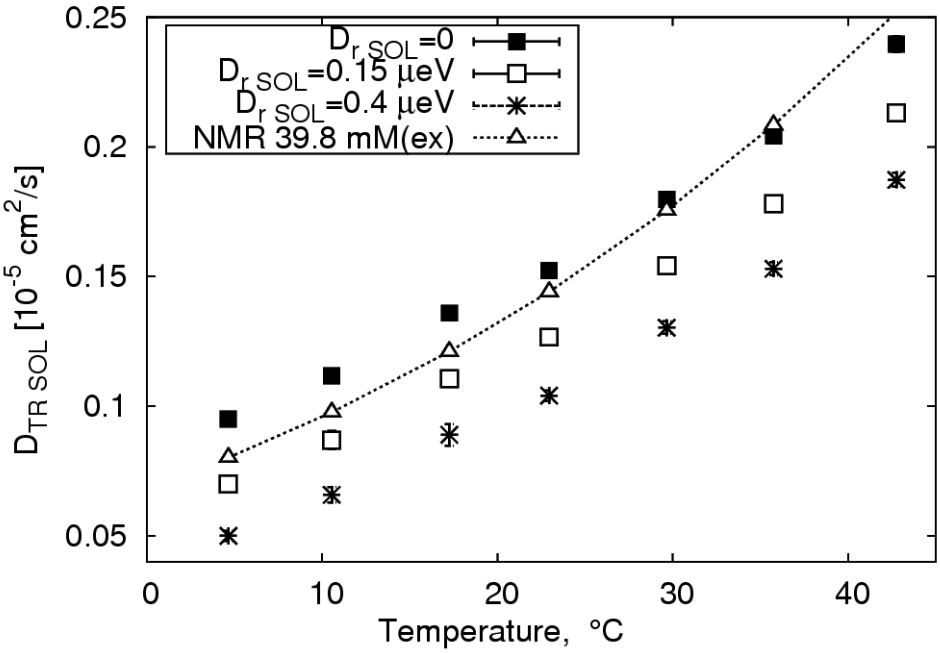

Figure 7.4 **Influence of the rotational diffusion coefficient, $D_{r\,SOL}$, (kept at various fixed values) on the translational diffusion coefficient, $D_{TR\,SOL}$, values determined from the fits of QENS spectra.** Fitted QENS spectra: {IN16} spectra of DIMEB solutions in D_2O with the concentration of 39.8 mM.

It is clear that the broadening due to rotational motion will increase with *Q*. The component with *l*=4 has already a rotational broadening (for $D_{r\,SOL}$ = 0.1 μeV) of 4.0 μeV (Tab. 7.3), so that the parameters of the rotational motion can, in principle, be determined from the {NEAT(3)} spectra of the D_2O solution with an energy resolution of ΔE≈10 μeV. An iterative approach can be used:

1) fitting the model to the {IN16} spectra with $D_{r\,SOL}$ = 0;
2) fitting the model to the {NEAT(3)} spectra with $D_{TR\,SOL}$ from step 1 and $D_{r\,SOL}$ being a free parameter;
3) fitting of {IN16} spectra with $D_{r\,SOL}$ being fixed to the value found in step 2;
4) et cetera.

Such an approach was attempted and led to $D_{r\,SOL}$ values in the range 0.4 -1 μeV and underestimated $D_{TR\,SOL}$ values.

Examples of the fits to the {IN16} spectra are shown in Figs. B1, B2, B3 (Appendix B).

One can see that already for the 3rd scattering angle (Fig. B2) the statistics is poor. Another feature is the substantial contribution from the container scattering, this contribution becomes more significant with decreasing the solute concentration (compare Fig. B1b and Fig. B3). Fits to the {NEAT(3)} spectra with $\Delta E \approx 10$ μeV are shown in Figs. B4, B5. Fig. B4b shows the decomposition of the solute component of the spectrum given by Fig. B4a into:

1. translational component, denoted as l=0;
2. sum of translational (l=0) and rotational (l=1) components, denoted as l=1;
3. sum of translational (l=0) and rotational components (l=1 and 2), denoted as l=2.

Fig. B5b shows the decomposition of the solute component of the spectrum given by Fig. B5a.

A fit of the "standard solute model" to {NEAT(3)} spectra for 0.51 Å^{-1} < Q < 0.74 Å^{-1} (and $D_{TR\,SOL}$ values fixed to the ones for DIMEB at 39.8 mM concentration from Tab. 7.4) resulted in the $D_{r\,SOL}$ values listed in Tab. 7.5. Applying an Arrhenius law to the first three points, one gets $D_{r\,SOL}$ =exp(-5.85-669/T), corresponding to an activation energy of 5.56 kJ/mol or 1.16 kcal/mol. Note that the values of $D_{r\,SOL}$ in Tab. 7.5 seem to be too high, judging by the estimate from eq. (7.2) and by available values for α and β-CD [7,9,94,137].

Table 7.5 **Values of the rotational diffusion coefficient, $D_{r\,SOL}$, of DIMEB-molecule found from the QENS spectra of DIMEB solution in D_2O c=50.0 mg/mL {37.6 mM}.** Fitted model: "standard solute model", fitted spectra: {NEAT(3)}, see Tabs. 3.1 and 3.2 for details.

t °C	$D_{r\,SOL}$ [μeV]
5.0	$0.26 \pm 1.0 \times 10^{-5}$
17.7	$0.291 \pm 1.2 \times 10^{-5}$
30.6	$0.318 \pm 1.3 \times 10^{-5}$
43.9	$0.173 \pm 1.6 \times 10^{-5}$

The main question regarding the results presented above is: why does the neglection of rotational motion when fitting {IN16} spectra result in apparently good $D_{TR\,SOL}$ values, while setting $D_{r\,SOL}$ to values, similar to those found in the literature, on the contrary yields $D_{TR\,SOL}$ values, which are underestimated?

7.6 The influence of the intermolecular structure factor

Qualitatively, it is clear from the results above that the contribution to the spectra originating from the rotational motion is smaller than predicted by the model employed. By revising the basis of the model, one can see that it is the intermolecular structure factor, $S_{SOL}(Q)$, which, being larger than unity, can result in an additional increase of the intensity of the translational component (and thus in an effective decrease of the contribution of rotation).

Indeed, the approximation $S_{SOL}(Q)$=1 is only valid when interactions between solute

molecules are weak and the solute concentration is small. In the small-angle scattering study (Chapter 6) it was found that for DIMEB and TRIMEG, $S_{SOL}(Q)$ is significantly larger than unity. Moreover, as it was seen in section 6.4, with increasing temperature and solute concentration, $S_{SOL}(Q)$ rises more drastically towards the low Q region.

The knowledge on how $S_{SOL}(Q)$ changes with temperature can be applied for the interpretation of the temperature dependence of the differences between QENS and PFG-NMR $D_{TR\,SOL}$ values shown in Fig. 7.2. For high temperature, and c=39.8 mM concentration of DIMEB, the value of $S_{SOL}(Q)$ is large, the neglect of rotational motion is *quasi* justified, and thus a good agreement is seen between values obtained by PFG-NMR and QENS. For the same concentration and low temperatures, the values of $S_{SOL}(Q)$ are probably smaller (correlated with the high solubility of DIMEB in cold water, see Chapter 6); thus, the neglection of rotational motion is justified to a lesser extent, and the agreement between QENS and PFG-NMR is therefore poorer. Naturally, because rotational motion leads to additional broadening of the shape of quasielastic peak, setting $D_{r\,SOL}$=0 leads to an apparent increase of the translational broadening, and, consequently, to an overestimation of the diffusion coefficients.

For 20.3 mM concentration of DIMEB, the reason for the discrepancy at low temperatures may be attributed to the same reason, as was done for 39.8 mM concentration. On the other hand, for the temperatures above 25 °C, one may anticipate that $S_{SOL}(Q)$ has a smaller importance than for 39.8 mM concentration, (for lower concentrations, the $S_{SOL}(Q)$ value is smaller, see Chapter 6). Thus, one could expect that the fit with $D_{r\,SOL}$=0 would result in an overestimation of the fitted values of the diffusion coefficients. However, the contrary is observed, and the reasons for this are not yet clear.

7.7 The importance of the knowledge of $S_{SOL}(Q)$ in the analysis of QENS spectra

Although further thorough investigation must be done regarding the influence of $S_{SOL}(Q)$ on the relative importance of the rotational motion in the analysis of QENS spectra, one can make some preliminary conclusions.

For a solution of a given substance, in case of the strong attractive solute-solute interactions (i.e. $S_{SOL}(Q)$ is substantially greater than unity), the translational diffusion coefficient of this substance can be found from QENS spectra of the solution, recorded with high energy resolution and for relatively low Q values. Measurements of the translational diffusion coefficient $D_{TR\,SOL}$ in concentrated solutions of proteins (or other molecules) by means of QENS might have advantages compared to other methods.

For substances which in solutions show repulsive solute-solute interactions, one should not neglect the contribution of rotational motion in the analysis of the QENS spectra taken at

low Q values and with high energy resolution. For $Q > Q_{MIN}$ ($Q_{MIN}=2\pi/D$, where D is the maximum diameter of the particle) the rotational components with non zero width will contribute substantially to the total broadening of the quasielastic peak. Neglecting rotational motion in such a case will lead to overestimated $D_{TR\,SOL}$ values.

Finally, in order to find $D_{TR\,SOL}$ or $D_{r\,SOL}$ values from the QENS spectra in the Q range where coherent scattering is appreciable (this must be judged by comparing the coherent and incoherent parts of $A_0(Q)$), one has to have at least some general knowledge on $S_{SOL}(Q)$. Alternatively, one can attempt to determine $D_{r\,SOL}$ from the Q_{EL} region of QENS spectra, where $S_{SOL}(Q)$ is nearly constant and close to unity (which - for molecules of the size of CDs - is probably true for $Q > 1$ Å^{-1}).

7.8 Intermediate and low resolution QENS spectra of DIMEB solutions in heavy water

The values of $D_{r\,SOL}$ determined by fitting the "standard solute model" to {NEAT(3)} spectra are unreliable for two reasons: a) the statistical accuracy of this particular experiment for $Q_{EL} > 0.5$ Å^{-1} was poor; b) the Q range as well as the maximum Q_{EL} value are small.

Tables 7.2, 7.3 show translational and rotational spectral broadenings and Fig. 7.3 shows $A_1(Q)$ values for DIMEB. It is clear that by fitting the model to the spectra for $Q > 1$ Å^{-1}, one should be able to obtain $D_{r\,SOL}$ with more certainty. In addition, $S_{SOL}(Q)$ is likely to be nearly constant and close to unity for $Q > 1$ Å^{-1}.

At first, fitting to the 90 μeV resolution {NEAT(4)} spectra of DIMEB was attempted, and a satisfactory description of the spectra by the "standard solute model" was obtained. However, it turned out that the sensitivity of the fit quality with respect to the $D_{r\,SOL}$ value was low, i.e. fixing $D_{r\,SOL}$ at values in the range 0.01 - 0.3 μeV had only little impact on the quality of the description of the spectra by the fitted curve.

Clearly, the {IN5(1)} spectra, owing to the higher resolution (30 μeV), allow a better separation of the solute and water motion. When the "standard solute model" was fitted to the {IN5(1)} spectra, it was found that the spectra could not be satisfactorily described by the fitted curve, see Fig. 7.5. Moreover, even for 5 °C the value of $D_{r\,SOL}$ determined in the fit was about 0.4 μeV and for 40 °C it was about 0.7-0.8 μeV. These values are too large in comparison to the $D_{r\,SOL}$ values available for β-CD and the $D_{r\,SOL}$ estimates performed according to eq. (7.2). Undoubtedly, the "standard solute model" fails in the case of DIMEB.

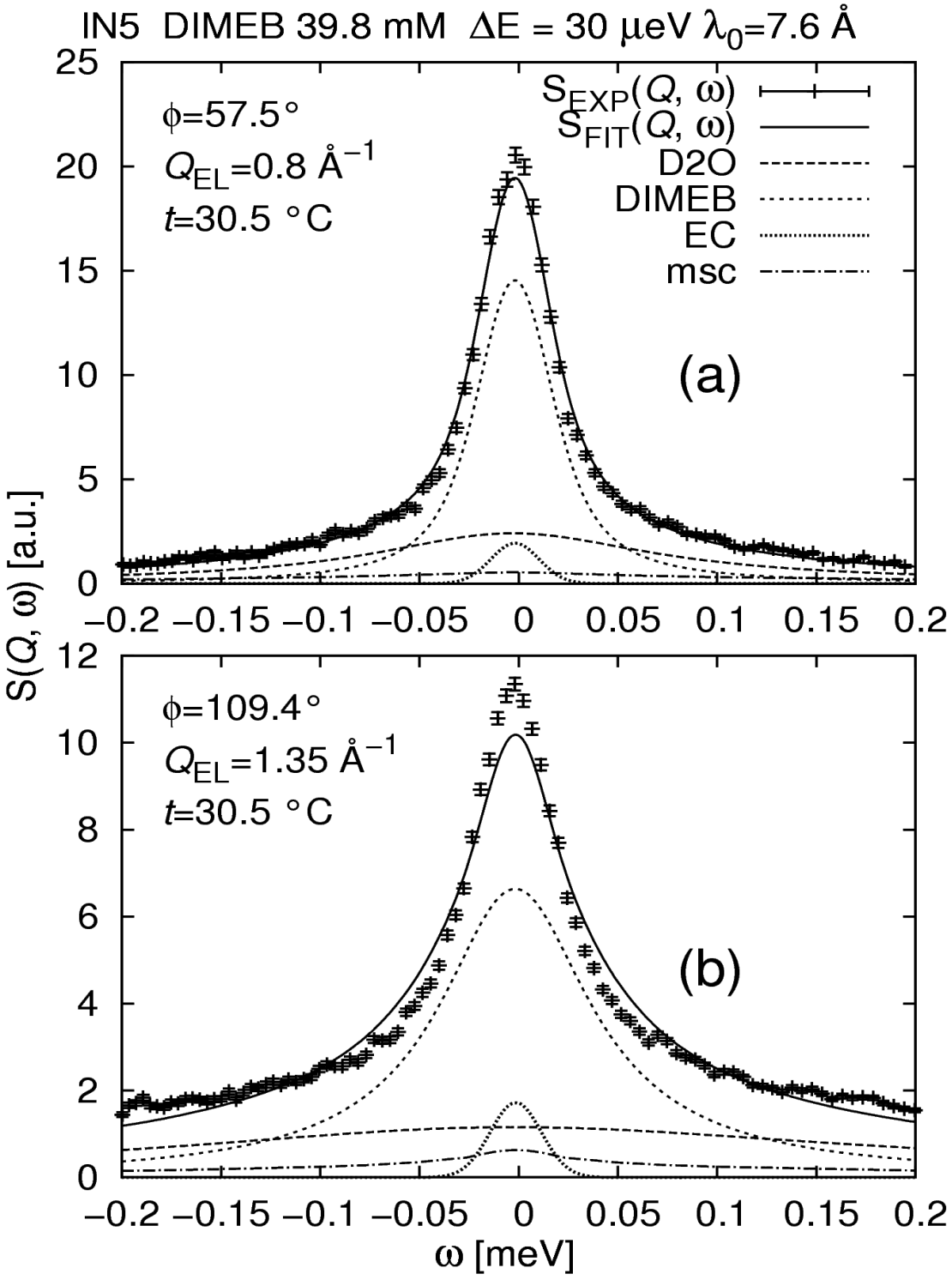

Figure 7.5 **Examples of fits of the "standard solute model" to spectra of DIMEB solutions in D_2O with the concentration 39.8 mM, ΔE≈30 μeV.** {IN5(1)} spectra for two scattering angles are shown, 57.5° and 109.4°. The total fitted curve: $S_{FIT}(Q, \omega)$; "D2O", "DIMEB" and "EC" represent the QENS components due to bulk D_2O, DIMEB, sample container scattering ($S_{SC\ EXP}$), respectively; "msc" is the multiple scattering component ($S_{MSC\ THEO}$).

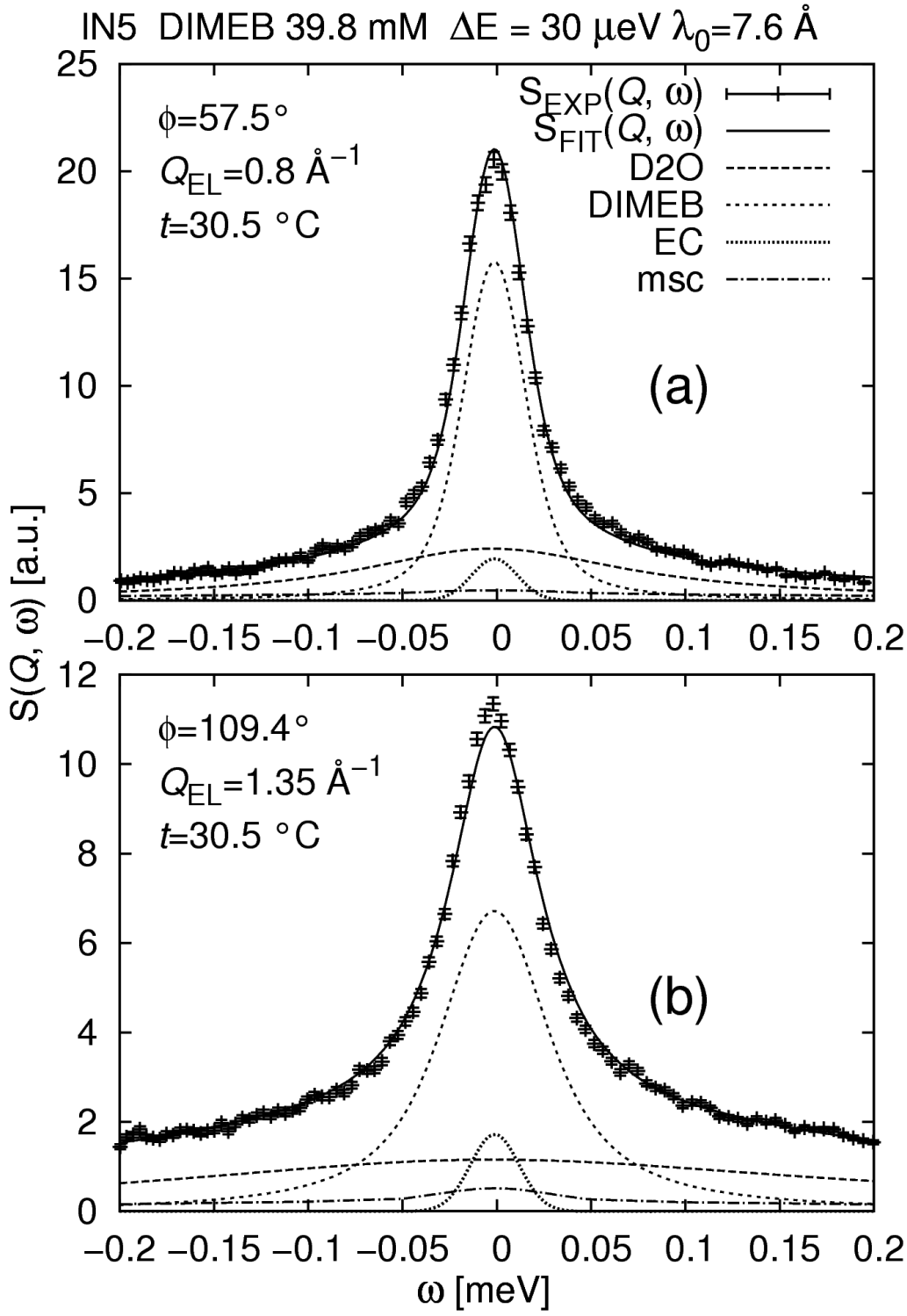

Figure 7.6 **Examples of fits of the solute model with the additional "broad" component to spectra of DIMEB solutions in D_2O with the concentration 39.8 mM, ΔE≈30 μeV.** {IN5(1)} spectra for two scattering angles are shown, 57.5° and 109.4°. By comparison with Fig. 7.5 a better agreement of the fitted curve with experimental data can be seen. The total fitted curve: $S_{FIT}(Q, \omega)$; "D2O", "DIMEB" and "EC" represent the QENS components due to bulk D_2O, DIMEB, sample container scattering ($S_{SC\ EXP}$), respectively; "msc" is the multiple scattering component ($S_{MSC\ THEO}$).

This Lorentzian component (called in the following "broad" component) may be due to the motion of -CH_3 and -CH_2-O-CH_3 groups (called "side" groups in the following). Indeed, the incoherent cross section of the DIMEB molecule in D_2O solution is ca. 8000 barn (see Tab. 5.1), and the hydrogens of methyl groups alone have a cross section of ca. 3500 barn (42 hydrogens × (σ_S=82) barn, see Tab. 2.1), i.e. a value consistent with the weight factor of the Lorentzian as determined in the fitting procedure (see below).

The addition of a Lorentzian to the expression for $S_{THEO\ SOL}(Q, \omega)$ corresponding to the "standard solute model", with the width and weight factor of the Lorentzian being fit parameters, allowed to obtain a good fit to the spectra (Fig. 7.6). The width was found to be about 0.25 meV - 0.50 meV, and the weight factor corresponded to a scattering cross section in the range of 3700 barn – 7500 barn.

From the point of view of its intensity, the "broad" component is unlikely to be due to the hydration water: the incoherent cross section of deuterium atom (Tab. 2.1) is equal to ca. 2 barn, so that 100 (for example) D_2O molecules would correspond to 400 barn (the incoherent cross section of oxygen is negligible). Even taking the total scattering cross section of D_2O molecule (which is ca. 20 barn, see Tab. 5.1) the contribution of 100 D_2O molecules would be only 2000 barn. The definite answer can be provided by the quantitative analysis of the correlation (if any) between the intensity of the unknown component and the number of methyl groups and the glucose residues per mCD molecule. Unfortunately, no measurements for other mCDs with 30 μeV (or similar) resolution are so far available, so that such an analysis has to be postponed to a future experiment.

It was tentatively assumed that the "broad" component is due to the rotation of the methyl group around O-CH_3 bond, and probably the rotation of the CH_2OCH_3 fragment around C-CH_2OCH_3 bond. It is not straightforward to describe the geometry of these motions, as a first step, therefore, the three-site reorientational jump model was used, see e.g. [8]. Such a model, although phenomenological, might be adequate at this stage of the analysis. Thus, two new fit parameters were introduced: the time between the successive jumps, τ_{FAST} and the radius of the circle of rotation, R_{FAST}, on which the three sites are located. Together with $D_{r\ SOL}$ there is a total number of three unknown parameters.

Fitting of the model to the {NEAT(4)} DIMEB spectra with the resolution 90 μeV only revealed that the good fit quality can be obtained with the values of τ_{FAST} in the range of 3 ps - 7 ps and R_{FAST} in the range of 3 Å - 7 Å. The {NEAT(3)} spectra with 10 μeV resolution are not well suited for the determination of the parameters of the motion of "side" groups, because the statistical accuracy is rather poor and the maximum Q_{EL} value is only about 0.8 $Å^{-1}$ (so that the resolution in real space is of the order of $2\pi/Q$ = 8 Å).

Fitting of {IN5(2)} spectra of DIMEB also did not allow to determine $D_{r\,SOL}$, τ_{FAST} and R_{FAST} unambiguously. One of the reason for this is that in these spectra the maximum Q_{EL} value was about 1.5 Å^{-1}, rendering the resolution in "real space" $2\pi/Q$ = 4 Å and thus making the unambiguous determination of R_{FAST} difficult.

A simplified, purely phenomenological approach was therefore chosen, where the motion of "side" groups was described by eq. (5.27), with the Q-dependent parameter $A_{MET}(Q)$ and the HWHM, W_{MET}. Results of the fits using such an approach are given in Figs. 7.7, 7.8. An Arrhenius fit of W_{MET} values (i.e. fit to the equation $W_{MET} = W_0 \times \exp\{- E_{a(FAST)}/RT\}$) gave W_0=3.56±0.06 [meV] and $E_{a(FAST)}$=11.46±0.16 kJ/mol. Comparing eq. (5.24) and (5.27) one finds (taking the motion to be due to jumps among three equivalent sites on a circle) τ_{FAST} [ps]= $0.6583 \times 3/W_{MET}$ [meV], so that the residence time between consecutive jumps is in the range from 7.9 to 4.4 ps.

The introduction of the additional component led to a change in the $D_{r\,SOL}$ values obtained in the fit to {IN5(2)} spectra of DIMEB. Now these values are closer to the estimates based on eq. (7.2), than the $D_{r\,SOL}$ values determined from the fit of the "standard solute model", thus giving indirect support for the relevance of the newly introduced component. Interestingly, for the highest temperature, $D_{r\,SOL}$ suddenly becomes smaller (Fig. 7.8). Moreover, in fits to the {NEAT(4)} spectra, the value of $D_{r\,SOL}$ first increases with temperature, but then starts to decrease, too (not shown).

Such a behavior of $D_{r\,SOL}$ may reflect stronger solute-solute interactions at elevated temperatures, (including formation of the transient oligomers) which might lead to a more hindered overall rotation of the single solute molecule. Nevertheless, it is clear that for the unambiguous determination of $D_{r\,SOL}$, and the geometry and dynamics of the -CH_3 (and -CH_2-O-CH_3) groups motion, future measurements with ΔE=30 μeV (or a similar resolution) and with Q_{EL} up to 3 Å^{-1} (or higher) will be required.

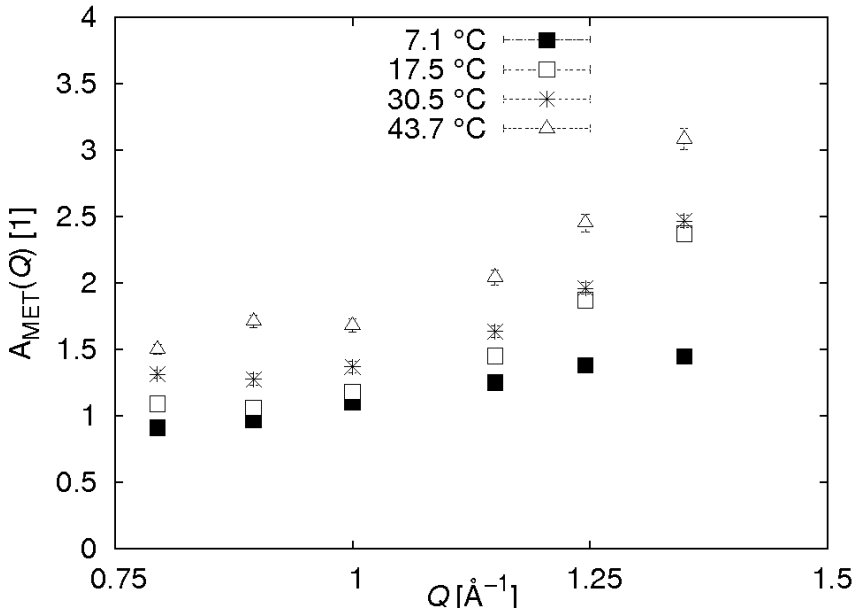

Figure 7.7 **The intensity of the component describing the motion of -CH_3 and -CH_2-OCH_3 groups, $A_{MET}(Q)$, as determined from the fit to the spectra of DIMEB solution in D_2O with the concentration 39.8 mM.** Fitted spectra: {IN5(1)}, ΔE≈30 μeV, see Tab. 3.2 for more details. The fitted model included the term for the description of the motion of -CH_3 and -CH_2-OCH_3 groups with two parameters, $A_{MET}(Q)$ and W_{MET} (the intensity and the width of the Lorentzian, respectively).

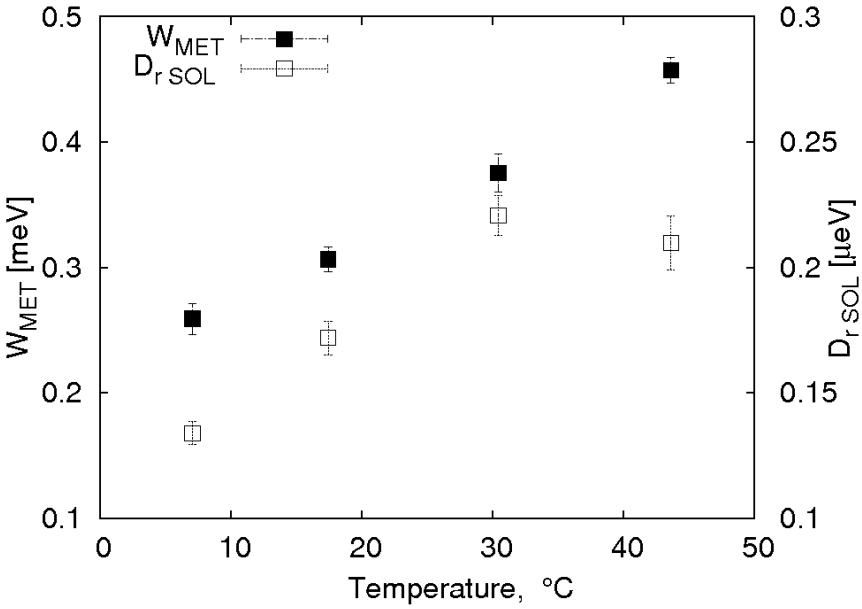

Figure 7.8 **Values of the rotational diffusion coefficient, $D_{r\,SOL}$, and the width of the component due to the motion of -CH_3 and -CH_2-OCH_3 groups, W_{MET}, as determined from the fit to the spectra of DIMEB solution in D_2O with the concentration 39.8 mM.** Fitted spectra: {IN5(1)}, ΔE≈30 μeV, see Tab. 3.2 for more details. The fitted model included the term for the description of the motion of -CH_3 and -CH_2-OCH_3 groups with two parameters, $A_{MET}(Q)$ and W_{MET} (the intensity and the width of the Lorentzian, respectively).

7.9 Scaling factor in fits of QENS spectra of DIMEB and TRIMEG solutions

In section 7.3 it was shown that the scaling factor Sc.F.(Q_{EL}) is fairly constant, if the scattering angle is far from the sample angle and if the model chosen to be fitted is correct. The "standard solute model" (see eqs. (5.11-5.17)) was fitted to the low Q region (0.1 Å^{-1} < Q < 0.5 Å^{-1}) of {NEAT(3)} spectra of γ-CD, DIMEB and TRIMEG solutions in D_2O. The resulting scaling factors Sc.F_{SOL}(Q_{EL}) together with the scaling factor from the fit to the D_2O spectra, Sc.F(Q_{EL}), are shown in Fig. 7.9. The weak decrease in the value of Sc.F(Q_{EL}) for D_2O at ≈0.4 Å^{-1} is due to the fact that the scattering angle is in the vicinity of the sample angle α (here: 60°). For γ-CD, instead of a dip, an increase in Sc.F_{SOL}(Q_{EL}) is seen, (due to some experimental problem; this sample leaked sometime later). Nevertheless, one can see that, outside the Q region with the imperfect correction, the values of Sc.F(Q_{EL}) for water and Sc.F_{SOL}(Q_{EL}) for γ-CD are about 200. On the contrary, for TRIMEG and DIMEB Sc.F_{SOL}(Q_{EL}) increases towards low Q. Moreover, in other experiments ({NEAT(4)}, {IN5(1)}) the same behavior of Sc.F_{SOL}(Q_{EL}) was observed for DIMEB (not shown). However, due to the larger value of the minimal accessible Q_{EL} value, (this value decreases with the incident wavelength) the relative increase in the Sc.F_{SOL}(Q_{EL}) values for mCDs is not as obvious in other experiments as it is in the case of {NEAT(3)} experiment with λ_0=15.3 Å.

Judging by the small-angle scattering results, one can attribute such a behavior of Sc.F_{SOL}(Q_{EL}) for DIMEB and TRIMEG to the fact, that the approximation $S_{SOL}(Q)$ = 1, employed in the "standard solute model", is not valid. However, while the increase of $S_{SOL}(Q)$ towards low Q can *qualitatively* explain the observed Sc.F_{SOL}(Q_{EL}) values, it can not explain it quantitatively. Indeed, for Q < 0.1 Å^{-1}, the values of $S_{SOL}(Q)$ found for DIMEB (Chapter 6) are smaller than 2, while in Fig. 7.9, the increase of Sc.F_{SOL}(Q_{EL}) (relative to the "normal" value of Sc.F_{SOL}(Q_{EL})≈200) is at least by a factor of 7.

Note that for Q < 0.35 Å^{-1} an influence of small errors in the values of $D_{TR\,SOL}$ fixed in the fit, as well as that of some small error in the values of $D_{r\,SOL}$, are not of great importance, because at such low Q values both translational and rotational broadening are negligible in comparison with the energy resolution of 10 μeV. (See Tab. 7.2 to compare the magnitudes of translational spectral broadening at Q < 0.35 Å^{-1} and ΔE=10 μeV. See Fig. 7.3 for l values with corresponding non-negligible rotational structure factors $A_l(Q)$ at Q < 0.35 Å^{-1}; and Tab. 7.3 for the rotational spectral broadenings for these l values.)

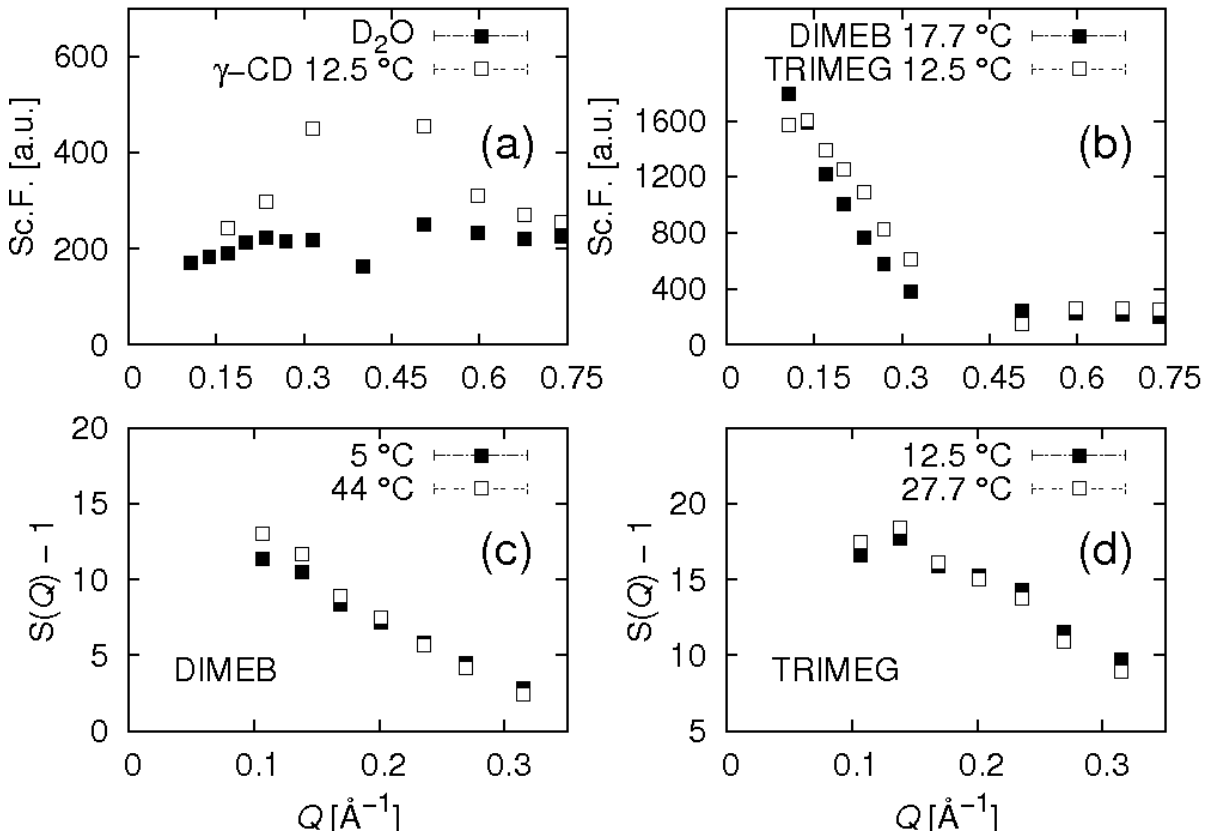

Figure 7.9 **Behavior of QENS intensity towards low Q region in the {NEAT(3)} spectra of D_2O and γ-CD, DIMEB and TRIMEG solutions in D_2O. (a):** scaling factor $Sc.F(Q_{EL})$ obtained in the fits to the spectra of D_2O & scaling factor $Sc.F_{SOL}(Q_{EL})$ obtained in the fits to the spectra of γ-CD; **(b):** $Sc.F_{SOL}(Q_{EL})$ from the fits to the spectra of DIMEB and TRIMEG; **(c) and (d):** values of $(S_{SOL}(Q) - 1)$ obtained from the fits of the "standard solute model" to DIMEB and TRIMEG spectra, respectively. Incident wavelength λ_0 =15.3 Å, ΔE=10 μeV, the concentrations of DIMEB, TRIMEG and γ-CD were 50.0 mg/mL {37.6 mM}, 61.4 mg/mL {37.6 mM} and 48.7 mg/mL {37.6 mM}, respectively.

It was attempted to fit the "standard solute model" to the {NEAT(3)} spectra of DIMEB and TRIMEG with the value of $\gamma_{CM\,SOL}(Q)$ (i.e. $S_{SOL}(Q) - 1$) being free and Q-dependent. Resulting values are presented in Fig. 7.9c,d. Such values are larger than those from the small-angle scattering results: see Fig. 6.5d for DIMEB.

Another explanation may be that the solute molecule has changed the conformation as compared to the crystal structure which was used to evaluate $A_{l(SOL)}(Q)$ from eq. (5.17). However, as shown by crystal structures, the per-dimethylated CDs are fairly rigid. Some distortions have been observed for the per-trimethylated CDs that lack the stabilizing hydrogen bonds O(3)-H···O(2) between adjacent glucoses. However, an observed great increase in $Sc.F_{SOL}(Q_{EL})$ can not be explained by the small conformational changes. It could be explained by the existence of oligomers, but no oligomers were observed in mCDs solutions, according to the results from small-angle scattering.

Therefore, it was speculated that an increase in $Sc.F_{SOL}(Q_{EL})$ values originates from a layer of D_2O molecules on the surface of methylated cyclodextrins. Such a layer would indeed result in the increase of coherent scattering from an mCD molecule and might explain the observed behavior of $Sc.F_{SOL}(Q_{EL})$.

7.10 Fits of the "hydrated solute model"

The "hydrated solute model" is described in section 5.8. The number of water molecules in the hydration shell (N_{HYD}) was the fitting parameter that was determined from a number of spectra. The results given in Fig. 7.10 show that N_{HYD} is about 70 for TRIMEG and about 60 in the case of DIMEB. For comparison, representing water molecules by spheres, it takes about 100 water molecules to form one homogeneous monolayer on the surface of a DIMEB molecule, this number being somewhat larger for TRIMEG.

The fact that the number of water molecules in the hydration shell of DIMEB and TRIMEG is "reasonable" (in particular, it is smaller than the number of water molecules required for the complete geometrical surface coverage) can be seen as a support for the assumption made in the present work. Namely, that the increase of the QENS intensity towards the low Q region (as observed in the spectra of mCD solutions in D_2O) is, at least partially, due to the coherent QENS component arising because of the significant correlations between the positions of water and solute molecules.

It is interesting to note that the N_{HYD} values found in the present study are similar to those obtained in a theoretical study [114] for DIMEB. Specifically, they found that a total of 46 water molecules at 25 °C and 31 water molecules at 70 °C belonged to the "hydrophilic hydration shell" (i.e. near –OH groups only) whereas in the "hydrophobic hydration shell" (i.e. near $–CH_3$ groups only) there were 147 water at 25 °C but 18 at 70 °C, per DIMEB-molecule.

Moreover, the analysis of the Fourier Transform Infra Red spectra of H_2O solutions of TRIMEB and TRIMEG resulted in the approximate number of hydration water molecules ≈ 70 per mCD-molecule [63]. (TRIMEB: c ≈210 mM, t = 10 °C; TRIMEG: c ≈150 mM, the temperature is not specified.)

In Fig. 7.10a,b one can see experimental and fitted values of $S(Q_{EL}, \omega=0)$. Remarkable agreement is observed for DIMEB; for TRIMEG the agreement is less good.

There are several factors which contribute to the difficulty of the application of the "hydrated solute model".

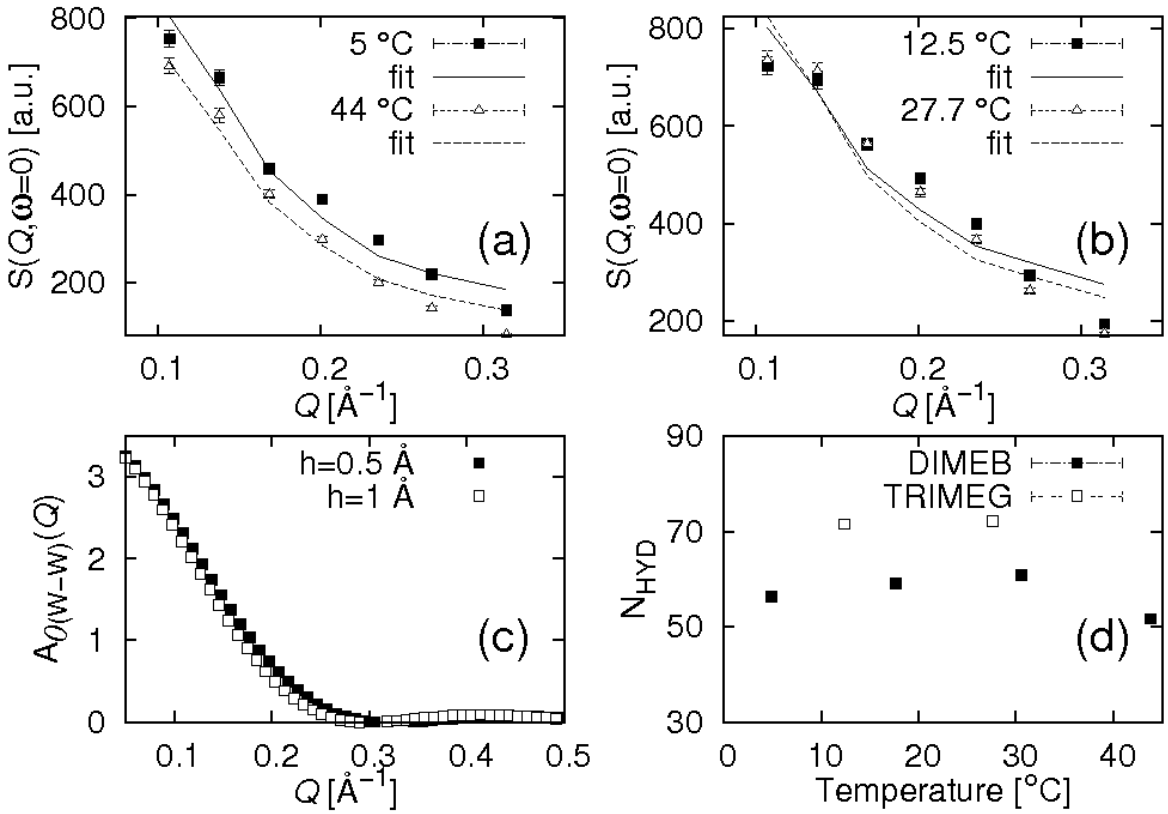

Figure 7.10 **Results of the application of the "hydrated solute model". (a) and (b):** Examples of the fit of the "hydrated solute model" to the {NEAT(3)} spectra of DIMEB and TRIMEG, respectively; **(c):** the dependence of $A_{0(W\text{-}W)}(Q)$ (part of the elastic structure factor of the hydrated solute molecule, $A_{0(mCD\text{-}HYD)}(Q)$) on the thickness of the hydration shell h; **(d):** the number of water molecules in the hydration shell (N_{HYD}) as determined in fits of the "hydrated solute model" to the {NEAT(3)} spectra of DIMEB and TRIMEG. Information on the {NEAT(3)} spectra: incident wavelength λ_0 =15.3 Å, ΔE=10 μeV, the concentrations of DIMEB and TRIMEG were 50.0 mg/mL {37.6 mM}and 61.4 mg/mL {37.6 mM}, respectively.

First, the rotational structure factors of the hydrated solute molecule, $A_{l(mCD\text{-}HYD)}(Q)$, are functions of N_{HYD} and h. In Fig. 7.10c one can see how $A_{0(W\text{-}W)}(Q)$ (one of the components of the elastic structure factor of the hydrated solute molecule, $A_{0(mCD\text{-}HYD)}(Q)$, see eq. (5.29)) changes with h. The parameter h is the thickness of the hydration shell (see section 5.8 and Fig. 5.1). Specifically, the distance between the center of the hydration water molecule (with radius R_{D2O}) and the center of the atom on the surface of the solute molecule (with radius R_{ATOM}) lyes between "h + R_{D2O} +R_{ATOM}" and "R_{D2O} +R_{ATOM}". At the present stage, the value of h was always fixed to 0.5 Å, but it is conceivable, that a better fit quality could be obtained, if h was fixed to a different value. It is, in principle, also possible to treat h as free fitting parameter (this poses difficulties in computation, however).

Fig. 7.10c also illustrates how rapidly the factor $A_{0(W\text{-}W)}(Q)$ decreases with Q

($A_{0(mCD\text{-}W)}(Q)$, another component of $A_{0(mCD\text{-}HYD)}(Q)$, decreases with Q in similar way). It is then clear that to observe the coherent scattering from the hydration shell (and to obtain reliable N_{HYD} values), QENS spectra at relatively low Q_{EL} values must be recorded. This, in practice, is only possible with TOF spectrometers, like NEAT and IN5, and by using a rather long incident neutron wavelength, which leads to the low incident neutron flux and relatively long measurement times.

Moreover, in fits of the "hydrated solute model" to the QENS spectra in the low Q region, it is difficult to obtain such an agreement as obtained, for example, in the description of the SAXS spectra of β- and γ-CD (Fig. 6.1). The QENS spectra are recorded conventionally for a small number of scattering angles (compared to that in small-angle scattering experiments). Correction of these spectra for the sample dependent attenuation factor is not easy (as opposed to SAXS/SANS). Other problems include the difficulty in converting the QENS spectra to the absolute scale (which is in fact required for obtaining N_{HYD} values).

It is clear that there must exist quasielastic scattering due to the spatial correlation between the solute and water molecules. Further tests of the "hydrated solute model" are therefore of great interest; these tests include the elucidation of the unusual behavior of $Sc.F_{SOL}(Q_{EL})$ and require the knowledge of the intermolecular structure factor $S_{SOL}(Q)$.

Potentially, the "hydrated solute model" allows to extract parameters of the hydration shell from the QENS spectra of *D_2O solutions*. Then, it would be an alternative to the study of the hydration shell employing the QENS spectra of *H_2O solutions*, which is not easy, in particular, for the simple reason given in section 7.13.

7.11 Small-angle scattering and QENS: different approaches to study hydration shell properties

For SANS and SAXS the central quantity is the scattering contrast, $\Delta\rho_{AV}$; $\Delta\rho_{AV} = \rho_{AV} - \rho_0$, where ρ_{AV} is the average scattering density of the solute molecule and ρ_0 is the scattering density of the solvent. The average scattering density of the hydration shell, $\rho_{AV\,HYD}$, differs from the scattering density of the bulk solvent, ρ_0, only due to a slight change in the number density of water molecules. In the study of the hydration shell of proteins in solution by means of SAXS and SANS the value of $\rho_{AV\,HYD}/\rho_0$ was found to be 1.06 – 1.2 [122]. However, as noted in the p. 1209 of reference [44], the density of hard spheres in contact with a hard wall would be higher than the bulk density of hard spheres by a similar factor. Thus, it is possible that the increase of $\rho_{AV\,HYD}$ compared to ρ_0 found in [122] was merely due to the packing conditions of the *bulk* water molecules at the protein surface. Then, such an increase reveals little about the hydration shell.

Quasielastic neutron scattering allows the observation of the hydration shell given that hydration water molecules are dynamically different from the bulk water molecules. In Figs. B1-B3 it is seen that the bulk water component is much broader than the solute component. Assuming that hydration water molecules diffuse together with the solute molecule during a finite time (the residence time of the water molecule in the hydration shell), the QENS component of hydration water will be narrower than the one of bulk water, but broader than the solute component. The width of the hydration water component may be used to determine this residence time. In case of D_2O solutions, the presence of the hydration shell leads to an increase of the QENS intensity at low Q, the magnitude of this increase can be used for the evaluation of the number of water molecules in the shell.

The relationship between the small-angle scattering and QENS and the differences between the two methods can be demonstrated using the concept of the observation time, Δt (see section 2.7).

In short, in the QENS experiment one measures:

$$S_{EXP}(Q, \omega) = S_{THEO}(Q, \omega) \otimes R(\omega) \tag{7.5}$$

where $R(\omega)$ is the experimental resolution function. For simplicity, it will be assumed that:

a) $R(\omega)$ is the Lorentzian with HWHM = $\Delta E/2$; ΔE is the energy resolution of the experiment;
b) the function $S_{THEO}(Q, \omega)$ is the sum of the contributions due to the bulk water, hydration water and solute molecules, $S_W(Q, \omega)$, $S_{HYDW}(Q, \omega)$ and $S_{SOL}(Q, \omega)$, respectively.
c) $S_W(Q, \omega)$, $S_{HYDW}(Q, \omega)$ and $S_{SOL}(Q, \omega)$ are proportional to Lorentzians with HWHMs of E_W, E_{HYDW}, E_{SOL}.

Then, eq. (7.5) can be rewritten as:

$$S_{EXP}(Q, \omega) = \{I_W(Q) \times Lor(E_W, \omega) + I_{HYDW}(Q) \times Lor(E_{HYDW}, \omega) + I_{SOL}(Q) \times Lor(E_{SOL}, \omega)\} \otimes Lor(\Delta E/2, \omega) \tag{7.6}$$

Applying the convolution theorem of Fourier transformation to eqs.(7.5, 7.6) yields:

$$I_{EXP}(Q, t) = I_{THEO}(Q, t) \times \exp(-t/\Delta t) \tag{7.7}$$

$$I_{EXP}(Q, t) = \{I_W(Q) \times \exp(-t/t_W) + I_{HYDW}(Q) \times \exp(-t/t_{HYDW}) + I_{SOL}(Q) \times \exp(-t/t_{SOL})\} \times \exp(-t/\Delta t) \tag{7.8}$$

where $t_i = 0.6583/E_i$, $\Delta t = 0.6583/(\Delta E/2)$; dimension of t_i and Δt: [ps]; ΔE and E_i: [meV].

In the small-angle scattering (diffraction) experiment the measured quantity is $I_{THEO}(Q, t = 0)$ (neglecting the finite Q resolution). For small-angle scattering (taking t=0), eq. (7.8) can be rewritten using the notion of the scattering contrast (see e.g. eq. (6.2) for the case when $I_{HYDW}(Q)$ is neglected). On the contrary, in the QENS experiment one has an access to the function $I_{EXP}(Q, t)$ given by eq. (7.8) either via the direct measurement or through the measurement of $S_{EXP}(Q, \omega)$.

By choosing an appropriate observation time Δt, one can achieve, e.g. that the term

$I_W(Q)\times\exp(-t\times(1/t_W+1/\Delta t))$ (bulk water contribution) will become very small. Alternatively, the term $I_{SOL}(Q)\times\exp(-t\times(1/t_{SOL}+1/\Delta t))$ can be made virtually equal to $I_{SOL}(Q)\times\exp(-t/\Delta t)$ (and thus independent on the solute dynamics) using the short observation time. By varying the observation time (the energy resolution) the contrast between the components due to dynamically different motions can be controlled (one might call it "dynamic contrast"). This allows, in principle, the determination of the parameters of different motions, given that the measurements with a number of various observation times were performed.

Finally, the integration of the QENS spectrum, (i.e. of the function $S(Q, \omega)$) over the energy transfer, $\hbar\omega$ for a given scattering angle φ, gives the QENS integral, $I_{QENS}(Q_{EL})$, see eq. (2.58). Ideally, the value of $I_{QENS}(Q_{EL})$ is equal to $I(Q_{EL})$, which is one single point on the small-angle neutron scattering curve. (But the approximate equality $I_{QENS}(Q_{EL}) \approx I(Q_{EL})$ holds only if the greatest part of $I_{QENS}(Q_{EL})$ originates from the region of energy transfers, where $k_0 \approx k$).

7.12 β-CD, TRIMEG and γ-CD

There is probably no significant influence of the intermolecular structure factor on the QENS spectra of β-CD: the concentration is small and, at least for γ-CD, $S_{SOL}(Q)$ was shown to be close to unity (as seen from the weak variation of $I(Q, c)$ with the concentration and temperature in Fig. 6.2). Thus, one could expect to be able to determine both $D_{TR\,SOL}$ and $D_{r\,SOL}$ values from the {IN16} spectra of β-CD.

The "standard solute model" was fitted to the 1 μeV resolution {IN16} spectra of β-CD. Invariably, the $D_{TR\,SOL}$ values determined in the fits were higher than the values found in the literature [75], see Tab. 7.6. The intensity of the scattering component due to β-CD is several times smaller than the solute component shown in Fig. B3 for DIMEB, (20.3 mM solution in D_2O); the low intensity of the β-CD scattering component is the main reason why the determined $D_{TR\,SOL}$ values are overestimated, and the $D_{r\,SOL}$ values are even more so.

The spectra of a β-CD solution recorded with 30 and 90 μeV resolution do not allow to determine $D_{r\,SOL}$ for the same reason. Thus, the investigation of the properties of aqueous solutions of β-CD by QENS is hindered by the low aqueous solubility of β-CD.

For TRIMEG, no values of the translational diffusion coefficients are available. An attempt was made to fit the $Q > 0.5$ Å^{-1} region of {NEAT(3)} spectra in order to obtain $D_{r\,SOL}$ values. To do that, $D_{TR\,SOL}$ values of TRIMEG were obtained from the $D_{TR\,SOL}$ values of DIMEB by correcting them for the difference in the volume of the molecule. It was then found for 12.4 °C: $D_{r\,SOL} \approx 0.18$ μeV, and for 27.8 °C: $D_{r\,SOL} \approx 0.31$ μeV. However, since no account for the motion of $-CH_3$ and $-CH_2-O-CH_3$ groups was made, these values are most probably overestimated.

For γ-CD, no $D_{TR\,SOL}$ values for the concentration 37.6 mM are available, so that no attempt to extract $D_{r\,SOL}$ values from the {NEAT(3)} spectra could be made.

For both γ-CD and TRIMEG, spectra with the intermediate energy resolution and sufficiently broad *Q* range have to be recorded in order to determine $D_{r\,SOL}$ and (for TRIMEG) the parameters of the motion of $-CH_3$ and $-CH_2-O-CH_3$ groups. Of course, an analysis of these spectra requires the knowledge of the translational diffusion coefficients for the concentrations studied.

Table 7.6 **Values of the translational and rotational diffusion coefficients, $D_{TR\,SOL}$ and $D_{r\,SOL}$, respectively, as determined from the QENS spectra of β-CD solution in D_2O.** Fitted spectra: {IN16}, the concentration of β-CD was 10.6 mg/mL {9.3 mM}; fitted model: "standard solute model"; dimensions: $D_{TR\,SOL}$ [10^{-5} cm^2/s], $D_{r\,SOL}$ [μeV].

T °C	$D_{TR\,SOL}$[a]	$D_{TR\,SOL}$[b]	$D_{TR\,SOL}$[c]	$D_{r\,SOL}$[c]	$D_{r\,SOL}$[d]
6.8	0.141	0.255±0.02	0.225±0.03	4.1±8.2	3.2±3.8
23.0	0.242	0.363±0.02	0.322±0.03	4.3±8.2	3.4±3.7
29.7	0.296	0.442±0.02	0.400±0.04	4.6±9.9	3.5±4.3
42.8	0.432	0.555±0.02	0.506±0.04	5.0±10	3.9±4.6

[a] Values are for 3.8 mg/mL in H_2O, taken from [75] and corrected for the difference in viscosity.
[b] Determined from the fit with $D_{r\,SOL}=0$.
[c] Determined from the fit with $D_{TR\,SOL}$ and $D_{r\,SOL}$ as free parameters.
[d] Determined from the fit with $D_{TR\,SOL}$ fixed to $D_{TR\,SOL}$ values from [a].

7.13 QENS measurements of D_2O versus H_2O solutions

In order to keep multiple scattering relatively small, the maximum sample thickness for H_2O solutions must be in the range from 0.2 to 0.4 mm, whereas for D_2O solution it can be up to 3 mm. This leads to the following considerations, which have to be taken into account when planning QENS experiment.

For high energy resolution, the greatest scattering contribution comes from the solute scattering component, because the solvent scattering component is simply too broad (e.g. Figs. B2, B3). The measured QENS intensity is proportional to the sample thickness. Therefore, for high resolution, the scattering intensity from the sample with H_2O solution will be up to 10 times lower (as opposed to the sample with D_2O solution and the same solute concentration). Consequently, one will have to either increase the measurement time or tolerate much poorer statistical accuracy.

For the low energy resolution, and for the low solute concentration and/or relatively low scattering cross section of the solute molecules, it is the bulk water scattering component which

dominates the QENS spectra of the solutions (this is especially often so in the case of the H_2O solutions). Therefore, (comparing to the spectra of D_2O solutions) although the usage of a thinner sample for H_2O solutions results in the decrease of the total QENS component by a factor of about 10, similar factor is gained back, because the scattering cross section of H_2O molecule is about 10 times greater than the one of the D_2O molecule.